

Journal Pre-proof



Impact of Sequencing Radiation Therapy and Immune Checkpoint Inhibitors in the Treatment of Melanoma Brain Metastases

Daniel A. Pomeranz Krummel, PhD, Tahseen H. Nasti, PhD, Benjamin Izar, MD, Robert H. Press, MD, Maxwell Xu, BS, Lindsey Lowder, DO, Laura Kallay, PhD, Manali Rupji, MS, Havi Rosen, BSc, Jing Su, PhD, Walter Curran, MD, Jeffrey Olson, MD, Brent Weinberg, MD, Matthew Schniederjan, MD, Stewart Neill, MD, David Lawson, MD, Jeanne Kowalski, PhD, Mohammad K. Khan, MD, PhD, Soma Sengupta, MD, PhD

PII: S0360-3016(20)30183-8

DOI: <https://doi.org/10.1016/j.ijrobp.2020.01.043>

Reference: ROB 26188

To appear in: *International Journal of Radiation Oncology • Biology • Physics*

Received Date: 8 August 2019

Revised Date: 15 January 2020

Accepted Date: 25 January 2020

Please cite this article as: Pomeranz Krummel DA, Nasti TH, Izar B, Press RH, Xu M, Lowder L, Kallay L, Rupji M, Rosen H, Su J, Curran W, Olson J, Weinberg B, Schniederjan M, Neill S, Lawson D, Kowalski J, Khan MK, Sengupta S, Impact of Sequencing Radiation Therapy and Immune Checkpoint Inhibitors in the Treatment of Melanoma Brain Metastases, *International Journal of Radiation Oncology • Biology • Physics* (2020), doi: <https://doi.org/10.1016/j.ijrobp.2020.01.043>.

This is a PDF file of an article that has undergone enhancements after acceptance, such as the addition of a cover page and metadata, and formatting for readability, but it is not yet the definitive version of record. This version will undergo additional copyediting, typesetting and review before it is published in its final form, but we are providing this version to give early visibility of the article. Please note that, during the production process, errors may be discovered which could affect the content, and all legal disclaimers that apply to the journal pertain.

© 2020 Published by Elsevier Inc.

**Title: Impact of Sequencing Radiation Therapy and Immune Checkpoint Inhibitors
in the Treatment of Melanoma Brain Metastases**

Running title: Radiation before immunotherapy enhances response

Daniel A. Pomeranz Krummel, PhD^{1‡}, Tahseen H. Nasti, PhD^{2‡}, Benjamin Izar, MD^{3†},
Robert H. Press, MD^{4†}, Maxwell Xu, BS^{1†}, Lindsey Lowder, DO⁵, Laura Kallay, PhD¹,
Manali Rupji, MS⁶, Havi Rosen, BSc¹, Jing Su, PhD⁷, Walter Curran, MD^{4,6}, Jeffrey
Olson, MD^{6,8}, Brent Weinberg, MD⁹, Matthew Schniederjan, MD⁵, Stewart Neill, MD⁵,
David Lawson, MD^{6,10}, Jeanne Kowalski, PhD¹¹, Mohammad K. Khan, MD, PhD^{4,6*} &
Soma Sengupta, MD, PhD^{1,12*}

¹Department of Neurology, University of Cincinnati College of Medicine OH.

²Department of Microbiology & Immunology, Emory Univ., Atlanta GA. ³Columbia
Center for Translational Immunology, Columbia University Medical Center, New York
City NY. ⁴Department of Radiation Oncology, Emory Univ. School of Medicine, Atlanta
GA. ⁵Department of Pathology & Laboratory Medicine, Emory Univ. School of Medicine,
Atlanta GA. ⁶Winship Cancer Institute, Emory Univ. School of Medicine, Atlanta GA.

⁷Department of Biostatistics and Data Science, Wake Forest School of Medicine,
Winston-Salem NC. ⁸Department of Neurosurgery, Emory Univ. School of Medicine,
Atlanta GA. ⁹Department of Radiology & Imaging Sciences, Emory Univ. School of
Medicine, Atlanta GA. ¹⁰Department of Hematology & Medical Oncology, Emory Univ.

School of Medicine, Atlanta GA. ¹¹Department of Oncology, LIVESTRONG Cancer Institutes, Dell Medical School, Univ. of Texas, Austin TX.

¹²University of Cincinnati Gardner Neuroscience Institute, Cincinnati OH.

‡Co-first authors; †Co-second authors; *Co-corresponding authors

Co-corresponding author information

Mohammad K. Khan, MD, PhD

Winship Cancer Institute, Emory University Hospital

1365C Clifton Road, Atlanta, GA 30322

Email: drkhurram2000@gmail.com

Tel: (404) 778-3473

Soma Sengupta, MD, PhD

Department of Neurology and Rehabilitation Medicine

University of Cincinnati Academic Health Center

PO Box 670525

Cincinnati OH 45267-0525

Email: soma.sengupta@uc.edu

Tel: (513) 558-2919

Conflicts of interest. Dr. Olson reports editorial consultancy for American Cancer Society. Dr. M. Khan reports a grant from Merck Pharmaceuticals, outside the submitted work. Dr. Sengupta reports advisory role for Novocure. Dr Lowder reports participating in Caris Life Sciences Molecular Advisory Board January 2020.

Authors responsible for statistical analysis. Statistical analysis of patient data was conducted by co-authors Manali Rupji and Jeanne Kowalski.

Data availability. Sequence data generated in this study has been deposited in GEO Bank (accession number GSE131521). The source data underlying Figs. 1a, 1b, 2, 3b, and Supplementary Fig. 1 are provided as a source data file. The source data file has been deposited in the Open Science Framework (OSF) repository under the unique identifier DOI TBD. The authors declare that all other data supporting the findings of this study are available within the main article and its Supplementary Information file or from corresponding authors upon reasonable request.

Funding. Financial support for the project came from: NIH-NINDS under award number NS083626 to S.S. (to support salary); Winship Cancer Institute Melanoma Philanthropic Funds to S.S. and M.K.K.; American Cancer Society Institutional Research Grant to M.K.K.; Department of Radiation Oncology, Emory Univ. Research Funds to M.K.K.; Merck Sharp & Dohme Corp. to M.K.K.; NIH-NCI K08-CA222663 and NIH U54-CA225088 to B.I.; the SITC-BMS Cancer Immunotherapy Translational Fellowship to B.I.; a Burroughs Wellcome Fund Career Award for Medical Scientists to B.I.; the

Ludwig Center for Cancer Research at Harvard to B.I.; Department of Oncology, LIVESTRONG Cancer Institutes, Dell Medical School, University of Texas at Austin, TX, Research Funds to J.K. Research reported in this publication was also supported in part by the Biostatistics & Bioinformatics and the Integrated Cellular Imaging Shared Resources of the Winship Cancer Institute of Emory University and National Institutes of Health/National Cancer Institute under award number P30CA138292. The content is solely the responsibility of the authors and does not necessarily represent the official views of the National Institutes of Health.

Impact of Sequencing Radiation Therapy and Immune Checkpoint Inhibitors in the Treatment of Melanoma Brain Metastases

Abstract

Purpose: Melanoma brain metastases (MBM) occur in ~50% of melanoma patients.

While both Radiation Therapy (RT) and immune checkpoint inhibitor (ICI) are used alone or in combination for MBM treatment, the role of combination and how these treatments could best be sequenced, remains unclear.

Methods and Materials: We conducted a retrospective analysis of patients with resected MBM who underwent treatment with either RT, ICI or a combination of RT and ICI. Among the latter, we specifically investigated the differential gene expression via RNA-sequencing between patients who received RT first then ICI (RT→ICI) vs. ICI first then RT (ICI→RT). We use a glycoprotein-transduced syngeneic melanoma mouse model for validation experiments.

Results: We find that for patients with resected MBM, combination of RT and ICI confers superior survival compared to RT alone. Specifically, we find that RT→ICI was superior compared to ICI→RT. Transcriptome analysis of resected MBM revealed that the RT→ICI cohort demonstrated deregulation of genes involved in apoptotic signaling, and key modulators of inflammation, most implicated in NFκB signaling. In a pre-clinical model, we show that RT followed by anti-PD-L1 therapy was superior to the reverse sequence of therapy, supporting the observations we made in patients with MBM.

Conclusions: Our study provides initial insights into the optimal sequence of RT and ICI in the treatment of MBM following surgical resection. Prospective studies examining

the best sequence of RT and ICI are necessary and our study contributes to the rationale to pursue these.

Journal Pre-proof

Introduction

Brain metastases are the commonest intracranial malignancy in adult cancer patients. Melanoma accounts for ~10% of brain metastases and ~50% of melanoma patients with advanced disease develop clinically overt melanoma brain metastasis (MBM). Recently, immune checkpoint inhibitors (ICI) produced intracranial response rates comparable to those previously described for extracranial systemic responses.¹⁻⁴ Notably, analysis of the MBM study was restricted to asymptomatic patients who did not require radiotherapy, neurosurgery, or steroids at time of enrollment. There is increasing pre-clinical and clinical rationale for synergistic effects of combining radiotherapy (RT) with ICI⁵⁻⁷; however, radiation dose and fraction size, and temporal sequence with ICI (before, concurrent, or after RT), remain unclear.⁸⁻¹⁰

Methods and Materials

Patient data. We conducted a retrospective analysis of patients from our institutional pathology database from 2010 to 2018 who had resection of a single MBM and received CNS-directed radiation therapy (RT) (n=8) or immune checkpoint inhibitor(s) (ICI) and RT (n=17) (Table 1; supporting source file). For patients with eligible samples, relevant clinical information was captured from the electronic medical record under an institutional review board (IRB) approved protocol (IRB00072396: "RAD2620-13: Melanoma Outcomes in Patients Receiving Radiation Therapy"). Patient characteristics captured included age at the time of brain resection, gender, presence of active systemic disease (defined as newly diagnosed metastatic disease and/or systemic progression within the last 3 months), presence of active extra-cranial metastases,

ECOG performance status, total number of brain metastases (including intact lesions), and melanoma molecular graded prognostic assessment (molGPA) score. Most patients received adjuvant RT after resection of the MBM (n=11) compared to resection for local progression after initial RT (n=6). Treatment characteristics included timing and use of systemic therapies (BRAF inhibitor and immunotherapy), extent of surgical resection (gross total or subtotal resection), and type of brain radiation (WBRT, SRS, or none). Type of radiation treatment was determined by the treating physician based on number of brain metastases per institutional practice. Both linear accelerator (LINAC)-based SRS and Leskell Gamma Knife (Elekta AB, Stockholm, Sweden) SRS were used based on the treating facility. The prescribed dose was determined per recommendations from Radiation Therapy Oncology Group (RTOG) 9005. WBRT was delivered using 3-dimensional conformal opposed lateral fields with multileaf collimation. The prescribed dose was determined per physician preference.

Survival analysis. Kaplan-Meier curves were created using the CASAS tool. CASAS is a GUI (R package) tool based on survival for comparing groups¹¹ A log-rank test was used to test for significant differences in survival. Univariate associations were estimated using the Cox proportional hazards model and Hazard ratios with 95% CI are reported. The significance level was set to 0.1 given the small sample size of the cohort.

RNA-sequencing. Patient tissue was obtained at time of surgical resection under IRB approved protocols. Tissue processing at time of surgery consisted of fixation in 10% neutral buffered formalin and routine overnight processing for permanent fixation and

paraffin embedding (FFPE: formalin fixed paraffin embedded). A retrospective search within the institutional pathology database from 2010-2018 for “melanoma” (including search fields restricted to brain specimens) yielded 79 specimens. Cases that did not have a sufficient amount of tumor volume for sequencing and did not receive radiation and/or immunotherapy were excluded. Samples were sent for sequencing at the Broad Institute Genomics Platform (Cambridge, MA, USA) that yielded acceptable sequence for analysis. Of the original 79 specimens, after exclusions only 17 samples met eligibility and had sufficient sequencing.

Tissue for light microscopy, immunohistochemistry and DNA molecular analysis were sectioned from the FFPE blocks at 5 μm thickness. Sections were stained using Hematoxylin (Richard-Allan Scientific 7211) and Eosin-Y (Richard-Allan Scientific 7111) for microscopic examination. Histopathologic tumor classification was reviewed by four board certified (American Board of Pathology) neuropathologists. After histopathologic review, unstained sections were submitted for DNA analysis, specifically SNaPshot mutational panel primer extension-based method (Thermo-Fisher) and Cancer Mutation Panel 26 (Illumina) per hospital protocol (see source file for Table 1). Unstained slides (5 μm thick, non-heat-treated) from FFPE tissue blocks were sectioned and area of interest macro-dissected by a board-certified neuropathologist using a corresponding H&E-stained slide. RNA was extracted (Qiagen, AllPrep FFPE kit), quantified, and quality measured by the DV200 score (fraction of RNA fragments whose length is >200 nts). Samples not meeting minimum requirements (≥ 750 ng RNA, preferred concentration 10 ng/ μL , DV200 > 0.3) were held for further evaluation. Samples were

processed and sequenced by Transcriptome Capture (Illumina HiSeq2500) at the Broad Institute (Cambridge, MA).

Gene expression analysis. Short-read sequences were aligned to the hg19 human reference genome using STAR (v2.4.1a). On average, we obtained 37,476,289 reads per brain metastasis sample. Feature counting with mapped bam files was used to obtain raw count files. SAMseq was used to conduct differential expression analysis, as it accounts for potential correlation in expression among genes and its permutation-based testing method was deemed more appropriate for a smaller sample size. After identifying differentially expressed genes (FDR cut-off, 0.05), expression levels were normalized with samrR before log₂ transformed.

Mouse experiments. B16F10 cell line and Lentiviral vector expressing Lymphocytic choriomeningitis Glycoprotein (GP) was transduced per manufacturer instructions (Clontech). B16F10-GP cells (5×10^5) were implanted in matrigel on right and left flank of 6-8 week-old female C57BL/6 mice (Jackson Laboratories) in accordance with Institutional Animal Care and Use Committee guidelines. After tumors were palpable (10 days), mice were irradiated on right side with a Superflab bolus (0.5 cm tissue equivalent material) placed over tumor, and thereafter tumor measurements taken. X-RAD 320 irradiation unit used a light beam ($<8 \text{ mm}^2$) focussed on tumor with mice under anesthesia. Tumor diameters were measured using calipers. Tumor volume was calculated using the formula for an ellipse (i.e. $4/3\pi \cdot (l \cdot w \cdot h)$, where l, w, h are three radii of the tumor taken perpendicular to each other).

Results

Immunotherapy and radiation timing. Patients with melanoma brain metastases (MBM) that received ICI and RT had superior survival compared to patients receiving RT alone (Supplementary Fig. 1). We stratified those patients who received ICI and RT into two treatment groups: (1) RT followed by ICI (RT→ICI) ($n=11$); (2) ICI followed by RT and then ICI again (ICI→RT) ($n=6$), where RT was either stereotactic radiosurgery (SRS), $n=15$; or whole-brain radiation therapy (WBRT), $n=2$. The median dose/fraction of SRS was 21 Gy/1 fraction (range 16-32.5 Gy in 1-5 fractions). WBRT was delivered in 30 Gy/10 fractions and 37.5 Gy/15 fractions, respectively. Survival analysis suggests that the RT→ICI treatment group had an improved outcome (log-rank $p=0.064$) (Fig. 1). At 15 months, we observe a separation in curves for the 'timing' analysis (Fig. 1), though the small sample size precludes our further testing the significance of this result.

Differential gene expression analysis. To gain insights into the potential benefits of sequencing RT→ICI vs. ICI→RT, we performed RNA-seq of the 17 included patients who received combination therapy of RT and ICI. Differential gene expression analysis of resected MBM between RT→ICI and ICI→RT treatment groups showed 48 deregulated genes (FDR cut-off 0.05), all increased in expression in the RT→ICI group (Fig. 2). Annotation/pathway enrichment analysis revealed a significant ($p<0.01$, Supplementary Table 1) enrichment of genes functionally involved in apoptosis and anti-apoptotic signaling, including: NIK (MAP3K14), key modulator of non-canonical NFKB signaling; RIPK1, a receptor interacting kinase which also participates in NFKB

as well as JNK and Akt signaling; DAB2, previously reported as down-regulated in ovarian cancer and has a role in immune regulation.

Sequential administration of α -PD-L1 and radiation *in vivo*. We next aimed to model the different sequences of RT/ICI combination therapy. We analyzed the clinical observation of improved outcome for RT \rightarrow ICI (for ICI, we used an anti-PD-L1 antibody) using the B16F10-GP syngeneic melanoma model (Fig. 3a). The best tumor control within the irradiated volume and non-irradiated region (the 'abscopal site') was noted for RT \rightarrow ICI (Fig. 3b), consistent with the observation in patients that RT \rightarrow ICI had improved outcomes (Fig. 1b). No anti-tumor activity was observed when CD8 T cells were depleted, indicating that T cells were necessary for responses to α -PD-L1 therapy in combination with RT (Supplementary Fig. 2).

Discussion

Our pilot study indicates that delivering RT followed by ICI may result in superior survival in MBM patients when compared to RT or ICI alone, or ICI followed by RT. In line with our study, several smaller studies indicate an acceptable toxicity profile of RT plus ICI and potentially improved responses in patients with MBM.¹⁵⁻¹⁷ Transcriptome analysis of resected MBM indicated changes in expression of a limited set of genes and pathway analysis indicates involvement of the NF κ B signaling pathway. In line with our observations, RT induces various mechanisms that may enhance response to subsequent therapy with ICI, including enhanced antigen presenting cells, induction of immune stimulatory cytokines and chemokines, enhanced T cell infiltration, induction of

immune stimulatory cytokine production by T cells, maintenance of T cell effector function, and partial reversal of T cell dysfunction.¹²⁻¹⁴ Of note, an important consideration when interpreting the RNA-seq data from this study is the timing of tumor resection and RT/ICI. The majority of evaluated specimens (11 of 17) were resected prior to adjuvant RT, suggesting that the differential gene expression may be more representative of intrinsic tumor biology than effects of prescribed therapies. However, the clinical outcomes still suggest sequential RT→ICI therapy results in improved anti-tumor responses and our murine model results support these clinical observations. A pre-clinical MBM model is needed to further functionally dissect the role of different sequencing strategies of RT and ICI.

In summary, our current study contributes to increasing evidence that sequencing RT and ICI may have differential impacts on the outcomes of patients with MBM and prospective studies to validate this are reasonable and necessary. We aim to design a prospective clinical study with sufficient patient numbers that would enable us to more fully explore this research and validate the results presented herein based on retrospective, small tissue samples.

References

1. Tawbi HA, et al. Combined nivolumab and ipilimumab in melanoma metastatic to the brain. *N Engl J Med* 2018;379:722-730.
2. Postow MA, Sidlow R, Hellmann MD. Immune-related adverse events associated with immune checkpoint blockade. *N Engl J Med* 2018;378:158-168.
3. Wolchok JD, et al. Overall survival with combined nivolumab and ipilimumab in advanced melanoma. *N Engl J Med* 2017;377:1345-1356.
4. Larkin J, Hodi FS, Wolchok JD. Combined nivolumab and ipilimumab or monotherapy in untreated melanoma. *N Engl J Med* 2015;373:1270-1271.
5. Dewan MZ, et al. Fractionated but not single-dose radiotherapy induces an immune-mediated abscopal effect when combined with anti-CTLA-4 antibody. *Clin Cancer Res* 2009;15.
6. Antonia SJ, et al. Durvalumab after chemoradiotherapy in stage iii non-small-cell lung cancer. *N Engl J Med* 2017;377:1919-1929.
7. Marconi R, Strolin S, Bossi G, Strigari L. A meta-analysis of the abscopal effect in preclinical models: Is the biologically effective dose a relevant physical trigger? *PLoS One* 2017;12: e0171559.
8. Chowdhary M, et al. BRAF inhibitors and radiotherapy for melanoma brain metastases: potential advantages and disadvantages of combination therapy. *Onco Targets Ther* 2016;9:7149-7159.
9. Patel KR et al. BRAF inhibitor and stereotactic radiosurgery is associated with an increased risk of radiation necrosis. *Melanoma Res* 2016;26:387-394.

10. Khan MK, Khan N, Almasan A, Macklis R. Future of radiation therapy for malignant melanoma in an era of newer, more effective biological agents. *Oncotargets Ther* 2011;4:137-148.
11. Rupji M, Zhang X, Kowalski J. CASAS: Cancer Survival Analysis Suite, a web based application. *F1000Research* 2017;6:919.12. Patel KR, et al. Two heads better than one? Ipilimumab immunotherapy and radiation therapy for melanoma brain metastases. *Neuro Oncol* 2015;17:1312-1321.
13. Buchwald ZS, et al. Radiation, immune checkpoint blockade and the abscopal effect: a critical review on timing, dose and fractionation. *Front Oncol* 2018;8:612.
14. Lumniczky K, Safrany G. The impact of radiation therapy on the antitumor immunity: local effects and systemic consequences. *Cancer Lett* 2015;356:114-125.
15. Hiniker SM, et al. A Prospective clinical trial combining radiation therapy with systemic immunotherapy in metastatic melanoma. *Int J Radiat Oncol Biol Phys* 2016;96:578-588.
16. Twyman-Saint VC. Radiation and dual checkpoint blockade activate non-redundant immune mechanisms in cancer. *Nature* 2015;520:373-377.
17. Tang C, et al. Ipilimumab with stereotactic ablative radiation therapy: phase I results and immunologic correlates from peripheral T cells. *Clin Cancer Res* 2017;23:1388-1396.

Figure Captions

Figure 1. Impact of timing. Kaplan-Meier curve of patients with melanoma brain metastases (MBM) who received radiation therapy (RT) and immunotherapy ($n=17$) stratified according to immunotherapy timing (immunotherapy before and after RT (ICI→RT) (cyan line, $n=6$) versus after RT (RT→ICI) (red line, $n=11$) (Table 1, Source file for Table 1). Hazard ratio (HR) based on Cox proportionality hazard models are reported as for ICI→RT vs RT→ICI group 3.54 (0.86-14.65), type 3 p -value = 0.0808, log rank p -value = 0.064.

Figure 2. Differential gene expression analysis. Unsupervised heatmap of differentially expressed genes (DEGs) (FDR < 0.05) of patients ($n=17$). DEGs all have identical q -values and are ordered based on decreasing fold change, so that RIPK1 has highest and IGKV3.15 lowest. All DEGs were overrepresented in the radiation therapy (RT) before immunotherapy (ICI) treatment group (RT→ICI) relative to the ICI before and after RT group (ICI→RT). Gene expression data are labeled by therapeutic regimen: ICI→RT (cyan line, $n=6$) versus RT→ICI (red line, $n=11$). Patient's gene expression followed unsupervised clustering based upon euclidean distance metrics and the complete linkage method. After unsupervised clustering, the dendrogram clustered the majority of patient treatment groups with each other. Each patient/column has been assigned a number and letter, shown at the bottom of the heatmap, to aid identification of the patient in the clinical table, e.g. Source file for Table 1.

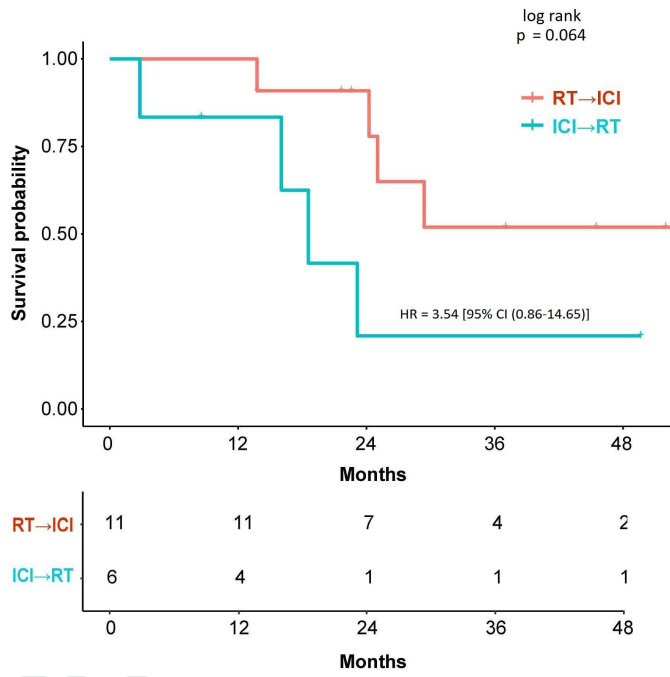
Figure 3. Radiation and α -PD-L1 response *in vivo*. **a** Mice implanted in left (L) and right (R) flanks with B16F10-GP cells received: (i) no treatment; (ii) α -PD-L1 alone; (iii) 10 Gy (right flank) on Day 10 (morning) before α -PD-L1 (RT \rightarrow ICI) (evening); (iv) α -PD-L1 first, followed by 10 Gy (right flank) on Day 20 (ICI \rightarrow RT). Sequence of α -PD-L1 and radiation is shown ($n=5$). α -PD-L1 antibody (200 μ g; clone 29F.1A12) was in phosphate buffer saline (500 μ L). **b** Mean tumor volumes of right and left tumors after different treatments (* $p<0.05$, ** $p<0.01$). Tumor measurements were taken with at least 5 mice per group (* $p<0.05$; ** $p<0.01$). Using ANOVA followed by Turkey, the two treatment groups have a p-value of 0.05 for the right side, while the left side they are not significantly different. Difference between the two treatment groups by T-test, the two groups are significantly different from one another on the right side ($p<0.001$), while left side p-value is 0.055.

Table 1 Abbreviated* melanoma brain metastasis patient data.

Variable	Level	N (%) = 17
Patient Characteristics		
Age (years)	Median (range)	54 (34-81)
Gender	Male	13 (76.5%)
	Female	4 (23.5%)
Race	White	17
Brain Metastases at Melanoma Diagnosis	Yes	6 (35.3%)
	No	11 (64.7%)
Active systemic disease	Yes	14 (82.4%)
	No	3 (17.6%)
Presence of extra-cranial disease	Yes	14 (82.4%)
	No	3 (17.6%)
Number of Brain Metastases	Median (range)	2 (1-6)
Pre-treatment LDH	Median (range)	202 (121-312)
<i>BRAF</i> mutation status	Mutated	9 (52.9%)
	Wild-type	8 (47.1%)
Melanoma molGPA	1-1.5	3 (17.6%)
	2.0-2.5	9 (52.9%)
	3.0-3.5	4 (23.5%)
	4.0	1 (5.9%)
Treatment Characteristics		
<i>BRAF</i> Inhibitor Use	Yes	5 (29.4%)
	No	12 (70.6%)
Immunotherapy Timing	After RT (RT→ICI)	11 (64.7%)
	Before And After RT (ICI→RT)	6 (35.3%)
Type of RT	SRS	15 (88.2%)
	WBRT	2 (11.8%)
RT Dose	SRS (dose/fractions)	Median (range) 21 (16-32.5)/1 (1-5)
	WBRT	Median (range) 33.75 (30-37.5)/12.5 (10-15)

*See Source file for detailed version of Table 1 patient data.

Journal Pre-proof



Journal Pre-proof

Figure 2

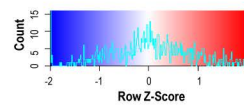
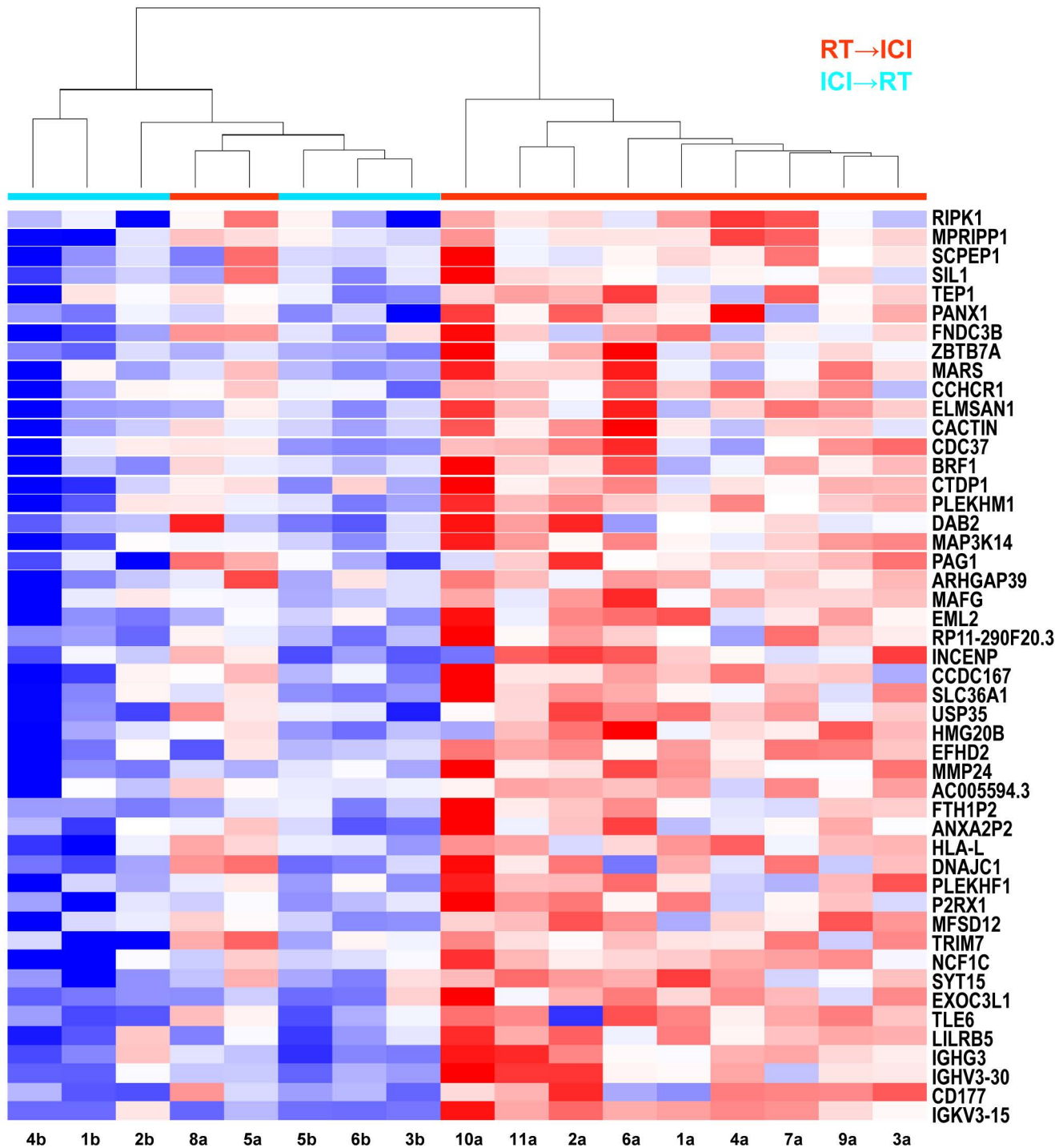
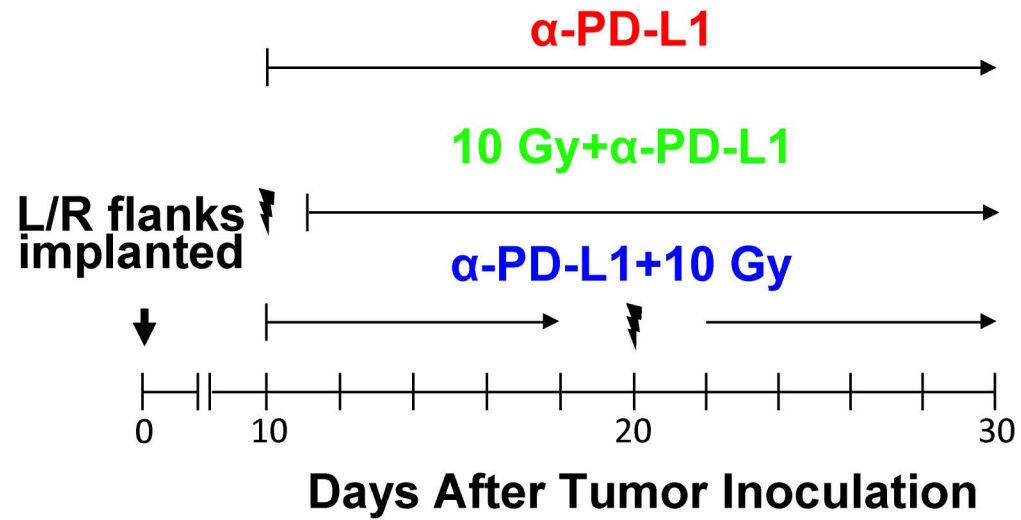
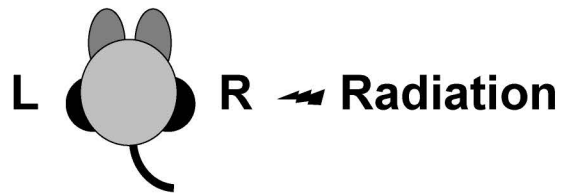


Figure 3**A****B**